Jurnal
Teknologi

Full Paper

FLEXURAL STRENGTH TEST OF PRECAST INDUSTRIALISED BUILDING SYSTEM BEAM-CORBEL CONNECTION

Chun-Chieh Yip[a*], Jing-Ying Wong[b], Xiao-Phen Lim[a]

[a]Department of Civil Engineering, Universiti Tunku Abdul Rahman, Bandar Sungai Long, 43000, Cheras, Kajang, Selangor, Malaysia
[b]Department of Civil Engineering, University of Nottingham Malaysia, 43500, Semenyih, Hulu Langat District, Selangor, Malaysia

Article history
Received
2 January 2019
Received in revised form
1 June 2019
Accepted
4 June 2019
Published online
26 August 2019

*Corresponding author
yipcc@utar.edu.my

Graphical abstract

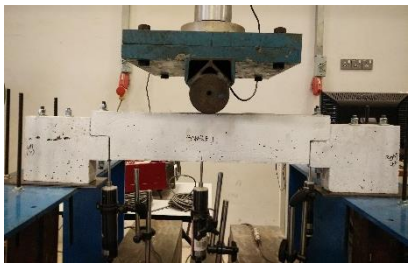

Abstract

Industrialised Building Systems (IBS) involves offsite fabrication in a systematic and controlled environment. The aim of this research is to determine the structural performance of newly enhanced column corbel support for IBS industry application. However, there is no solid data to support the industry in producing safe and reliable IBS structure with newly enhanced prototype. Hence, the objectives of this research paper are to identify failure behaviour, flexural strength, maximum deflection and ductility of the IBS beam to column corbel connection. Scaled 1:5 IBS beams with column supports were prepared according to Buckingham and Similitude Theorem. Result contribution of five specimens were obtained from the flexural strength test. The scaled beam has maximum flexural resistance of 2.2 kNm and deflection of 7 mm. The projected flexural resistance for full scale beam is 1265.6 kNm with ultimate load deflection of 35 mm. Failure behaviours such as shear cracking, flexural cracking and concrete crushing have been identified. The average ductility of the specimen was 3.23 which is higher than 3.0 from PCI design handbook. The newly improved specimen has the load bearing improvement of 32%. Thus, this research has positive outcome that could improve the confident level of the industry user toward this product.

Keywords: Industrialised building systems, precast reinforced concrete beam, flexural strength test, Similitude Theorem, scaled model

Abstrak

Sistem Bangunan Berindustri (IBS) melibatkan fabrikasi luar tapak di dalam persekitaran yang sistematik dan terkawal. Tujuan penyelidikan ini adalah untuk menentukan prestasi struktur korbel tiang baru yang dipertingkatkan untuk aplikasi industri IBS. Walau bagaimanapun, tidak ada keputusan konkrit untuk menyokong industri dalam penghasilan struktur IBS yang selamat dan boleh dipercayai dengan prototaip baru yang dipertingkatkan. Oleh itu, objektif kertas penyelidikan ini adalah untuk mengenal pasti tingkah laku kegagalan, kekuatan lenturan, pesongan maksimum dan kemuluran IBS pada sambungan rasuk ke tiang. Rasuk IBS berskala 1:5 dengan sokongan tiang telah disediakan mengikut Teori Buckingham dan Similitude. Sumbangan hasil keputusan lima spesimen telah diperolehi daripada ujian kekuatan lenturan. Rasuk berskala mempunyai rintangan lentur maksimum 2.2 kNm dan pesongan 7 mm. Rintangan lenturan untuk rasuk berskala penuh yang dianggarkan adalah 1265.6 kNm dengan pesongan beban muktamad 35 mm. Tingkah laku kegagalan seperti retak ricih, retakan lenturan dan penghancuran konkrit telah dikenalpasti. Nilai kemuluran purata spesimen adalah 3.23 kali lebih tinggi daripada 3.0 daripada buku panduan reka bentuk PCI. Spesimen baru yang diperbaiki mempunyai peningkatan beban sebanyak 32%. Oleh itu, kajian ini

mempunyai hasil positif yang dapat meningkatkan tahap kepercayaan para pengguna industri terhadap produk ini.

Kata kunci: Sistem binaan berindustri; rasuk konkrit bertetulang pratuang; ujian lenturan; Teorem Similitude; model berskala

1.0 INTRODUCTION

The world is moving fast towards sustainable development. With the sustainable development, the nation will have effective economic growth, high quality living environment, waste minimization and conservation of resources [1]. Besides, sustainable development in conjunction with industry 4.0 in Malaysia has caused the construction industries moving towards automation. With the effective building component fabrication through pre-cast or Industrialised Building System (IBS), wastage could be reduced and improved technological usage in industry [2].

The term Industrialised Building System (IBS) defines the construction process done off site or in factory under strict quality control with minimal construction site activity. The IBS components such as slab, beam, wall, column and staircase are pre-fabricated from the factory. These IBS components are able to be assembled together to become a complete structure on construction site. Therefore, the building components has to be planned, and manufactured accurately [3].

In addition, construction industries that adopts the IBS technology are able to minimize their labour on site and maximize the production output by giving more training opportunities to their workers to enhance the technical skill in factory [3]. According to The Construction Industry Development Board (CIDB) in Malaysia, IBS are categorized into five different type shown as follow [4].

1. Block work system,
2. Prefabricated timber framing system,
3. Steel formwork system,
4. Pre-cast concrete system
5. Steel framing system

The pre-cast concrete system consists of the precast concrete components such as pre-cast beam, girder beam, pre-cast column, slabs and wall components to construct a structure [5]. Construction Research Institute of Malaysia has asserted that pre-cast components may have various shapes for different purpose and type of usage. The functionality of the pre-cast shapes and usage have to comply both architectural and structural aspect [6]. The pre-cast functionality and usage for this research paper is focus in the semi-rigid joint connection with the newly enhanced column corbel with the IBS beam component published by previous research [7-9].

Concrete is a rocklike non-homogeneous material. Concrete can be produced by mixing four basic ingredients such as coarse aggregates, fine aggregates, cement powder and with the reaction from water [10]. Concrete mixes may have different proportion and extra chemical admixture to obtain the desired strength, workability and concrete hardening duration [11]. Apart from that concrete chemical admixture or sustainable material as raw material replacement may provide better quality and low carbon emission concrete for various applications [12].

The research paper adopts the Self-Compacting Concrete (SCC) for congested reinforcement environment. SCC was found by Professor Hajime Okamura of Kochi University of Technology, Japan, in 1986. According to Okamura (2003), SCC has high workability that can be compacted into every corner of the formwork easily by fresh concrete own self weight or gravitational attraction without the need from vibrating compaction [13].

The study of this research paper is focusing in both the flexural strength and ductility of the components. In structural design aspect, adequate capacity should be incorporated into the design to provide optimum safety for unforeseen overloaded scenario typically for newly innovated pre-cast component with unique connection [14].

The concept of ductility in the structure measures capacity of the structural system and its components to deform before total collapse, without a substantial loss of strength. High ductility beam provides a better chance of survival when the structure is overloaded, accidental impact or severe earthquake [15]. According to research done by Yip *et al*., 2017 [16] this beam to column joint has been used to construct the seismic resistance building. However, previous research discovered the column corbel connection is weak in resisting vertical load and caused plastic hinge easily. Therefore, this is an important indicator for initiating the study of an improved IBS beam to column joint connection.

Since the model done by Yip *et al*., 2017 [16] fulfils the strong column weak beam theory, but the strength of the connection between both column and beam must not be overlooked. Strong column weak beam theory defines the moment resistance of the column, M_{cy} should be higher than the flexural strength of beam, M_{by} [7]. Thus, the risk for formation of plastic hinge could be reduced or formed on beam support rather than column corbel support.

Small scale models have been frequently used by many researchers to investigate the behaviour of the full-scale model. However, researchers are always

having issues between the ultimate capacities of down scaled model in comparison with full scale model.

Many researchers are using Buckingham and similitude theories in investigating the scaled structural performance and capacities due to insufficient testing facilities for full scale model. Therefore, down scaled model is the only viable option and economical way to perform an experimental test [8].

Similitude law is a mathematical technique to integrate the theoretical relation of variable to describe the physical phenomenon [9]. The fundamental of the similitude law requires dimensionally homogeneous relations in forming any equation.

The common dimensions in physical models are length (L), force (F), mass (M) and time (T). The scaled and full scale relations are valid provided the equation is dimensionally homogeneous regardless of the units used for physical variables [9]. In short, the full scale equation and scaled model equation must be in equilibrium state. A scale factors S_i is introduced to achieve this equilibrium state.

Buckingham's π Theorem describes any dimensionally homogeneous equation involving in physical quantities can be expressed as an equivalent equation involving a set of dimensionless parameters [9]. The concept starts with initial equation f(X_1, X_2, X_3, …X_n) has X_i physical variables are equivalent to another equation g($\pi_1, \pi_2, \pi_3, \ldots \pi_m$) with same dimensional parameters as initial equation plus a different variables π_i = X_{ka}, X_{lb}, …X_{mc} to form equilibrium between both equations. In short, normal equations can be overwrite into another new equations for other application by changing the internal equation's physical variables factor. Hence, with the combination of Buckingham's π Theorem and similitude law, the prototype structure (p) full scale and the scaled model (m) can be distributed into simple equation as shown in Equation 1.

$$\pi_i^p = \pi_i^m \quad (1)$$

Prototype and scaled structural model capacity is controlled by scale factors S_i [9]. Scale factor S_i is defined as quantity Q in prototype model over quantity Q in model as shown in Equation 2. The quantity can be any homogeneous dimensions.

$$S_i = \frac{Q_p}{Q_m} \quad (2)$$

The useful quantified scale factors for common engineering purpose are shown in Table 1. Scale factors S_i in every equation must take into consideration for obtaining scaled model capacity or prototype capacity. Scale factor *S* is dimensional scale factor such as height, thickness, width and length [17].

Scale factor S_e is equivalent to elasticity of $E_{prototype}$ over elasticity of E_{model} which defines the downscaled material strength effects under structural material elasticity [18].

Last but not least, the scale factor in acceleration domain S_a = [(1/$S^{1/2}$)(S/$S^{1/2}$)] = time multiplication with velocity dimension = 1.0 in constant gravitational environment [17]. The acceleration domain may change subjected to different gravitational pull such as in the space, in different planet and under the sea. Therefore, careful application of these scale factors in conducting scaled specimen test to obtain structural behaviour and performance is feasible.

Table 1 Similitude relations for elastic model

Parameter	Scale factor
Dimension (h_p = Height or t_p = Thickness)	S
Area A_p	S^2
Volume V_p	S^3
Linear displacement U_p	S
Moment of inertia I_p	S^4
Frequency *f*	$S^{-1/2}$ or $(S/S_a)^{-1/2}$
Time	$(S/S_a)^{1/2}$
Density ρ_p	S_e/S_aS
Point load F_p	S_eS^2
Line load F_L	S_eS
Uniform distributed load P_p	S_e
Shear force V_p	S_eS^2
Moment *M* or Torque *T*	S_eS^2
Stress σ_p	S_e
Velocity *V*	$(S)^{1/2}$
Acceleration *a*	S_a or $S/S = 1$
Curvature *C*	$1/S$
Mass *M*	S_eS^2/S_a
Stiffness *K*	S_eS
Spectral Acceleration S_A	$S_eS^2/(S_eS^2/S_a)$

IBS reinforced concrete beams and column corbel support components were constructed to perform the flexural strength test. The aim of this research is to determine the structural performance with the newly enhanced column corbel support for IBS industry application. The contribution of this research is to understand the new prototype of the IBS system performance and provides better understanding to the industry stakeholder before commercialization. However, there is no solid data to support the industry in producing the safe and reliable IBS structure with newly enhanced prototype. Hence, the objectives of this research paper are to identify failure behaviour, flexural strength, maximum deflection and ductility of the IBS beam to column corbel connection. The beam sample reinforcement detailing and concrete mix proportion of the specimens are design based on the previous research done by Yip *et al*., 2015 & 2016 [19] & [20]. The specimen is scaled to 1:5 in accordance to the Bucklingham and similitude theorem S = 5.0, S_e = 4.5 and S_a = 1.0 introduced by Yip *et al*., 2017 [16]. This is because the current enhanced column corbel model is referred from the primary model done by previous researchers. Apart from that, the purpose of conducting the scaled model is due to the limited resources and available facilities in the University.

2.0 METHODOLOGY

2.1 IBS Beam-Corbel Reinforcement Specification

Figure 1 shows the overview of the reinforced concrete IBS beam and new enhanced column corbel specimen configuration. This is a scaled 1:5 model. The IBS beam has an existing steel anchor plate at both ends. Those IBS beam with anchor plate is used to join the column corbels by bolt and nuts together. The basic full scale capacity of this IBS beam was checked with accordance to European Code 2 [21].

The scaled 1:5 IBS beam has total length of 500 mm with clear span of 420 mm as shown in Figure 2. There are 40 mm length from both sides of the IBS beam used for the joint connection. This IBS beam has 100 mm in depth and 40 mm width. The diameter of main reinforcement and shear links are 5 mm and 1.5 mm respectively. The minimum yield stress, f_y of the main reinforcement is 500 MPa based on European Code 2 seismic resistance requirement [21]. The shear links were fabricated in continuous spiral loops. The continuous spiral loops can act as an internal damping system for seismic energy dissipation and shear resistance improvement [20].

Besides, there are two steel anchor plates embedded in the beam and column corbels surrounding the bolt holes. The purposes of steel plate anchor plates are to grip the bolts and nuts together and prevent the beam from falling apart when the beam-column concrete joint damaged. In previous study done by Yip *et al.*, 2016 [20], the IBS beam has anchor plate while column corbel does not equipped with any anchorage plate to protect the join connection. This has resulted the failure of joint happened around the column corbel rather than IBS beam itself. To mitigate this issue, an additional steel anchor plate with 2 mm thickness in the column corbel was introduced to secure the joint support.

Apart from that, T-blocks column component was constructed to support IBS beam. The anchorage joint connection together with bolt and nut in full scale capacity were checked with accordance to European Code 3 [22] and British Standard BS5950 [23]. Thereafter, everything was scaled to 1:5 except material strength. The reinforcement in column block utilized is 3 mm in diameter steel bar with yield strength, f_y of 500 MPa.

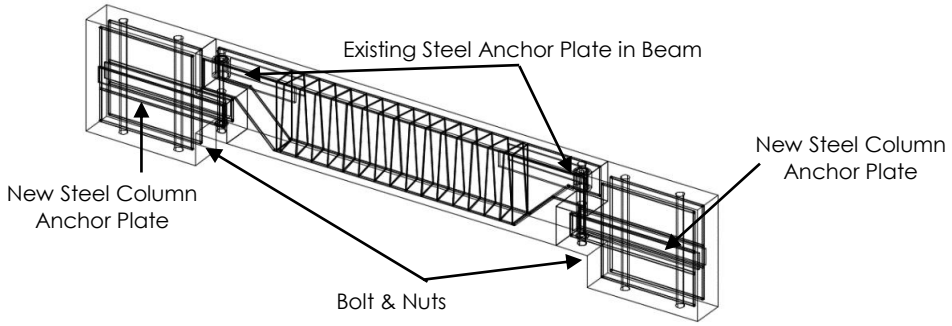

Figure 1 3D View of IBS beam-column corbel support

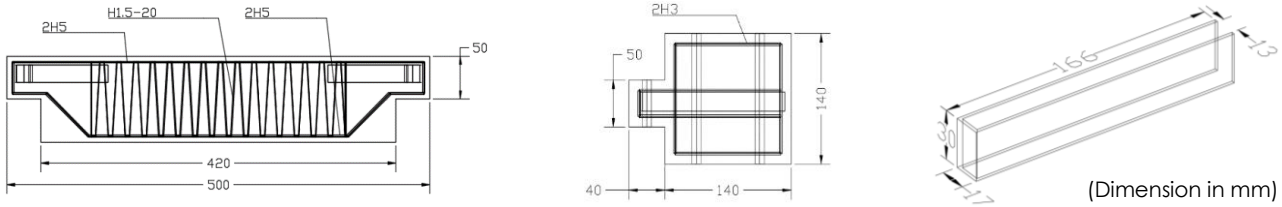

Figure 2 Detailing of (a) Beam, (b) T-block Column & (c) New Steel Column Anchor Plate

2.2 Concrete Mix Specification

Concrete Grade C30/37 concrete mix was used to prepare the specimens. Table 2 shows the mix proportions for concrete done by Yip *et al.*, 2016 & 2017 [16] & [20]. The concrete mix has density of 2380 kg/m^3 for this particular mix proportions and the mix design is based on the British Standard BS5328 [24].

The coarse aggregate with size 3 to 5 mm in diameter was utilized in the concrete mixture due to the congested reinforcement and 5 mm nominal cover of scaled specimens. The 6.6 kg/m^3 super plasticizer with brand Glenium 8008 was measured based on 1.2 % of cement powder. With the addition of the super plasticizer into the fresh concrete, the workability of fresh concrete was improved tremendously and results in high early hardening strength.

Table 2 Mixture of concrete

Grade C30/37 Concrete Mix Proportion	
Water / Cement ratio	0.42
Cement, kg/m^3	550.0
Water, kg/m^3	233.0
Fine Aggregate, kg/m^3	511.0
Coarse Aggregate, kg/m^3	1086.0
Density, kg/m^3	2380.0
Glenium 8008, kg/m^3	6.60

Eight concrete strength control cylinders with size 100 mm in diameter and 200 mm height were casted for the compressive strength test. Four concrete cylinders were tested for 7 days compressive strength while another four concrete cylinders were tested for 28 days compressive strength. The summary of tested result is shown in Table 3. The average concrete compressive strength for 7 days strength and 28 days strength were 27.14 N/mm^2 and 32.97 N/mm^2, respectively. This grade C30/37 mixture with super plasticizer managed to achieve 27.14 N/mm^2 > 24 N/mm^2 which beyond 80% of the desired compressive strength in 7 days. The mixture of this concrete grade C30/37 mixture is very promising for industry and the mixture could achieve 32.97 N/mm^2 compressive strength at 28 days.

Another eight concrete cylinders with same size were casted for the splitting tensile strength test. Four concrete cylinders were tested for 7 days splitting tensile strength and another four concrete cylinders were tested for 28 days splitting tensile strength. The summary of tested result is shown in Table 4. The average concrete tensile splitting strength for 7 days strength and 28 days strength was 2.93 N/mm^2 and 3.23 N/mm^2, respectively. The concrete samples satisfied the desired tensile splitting strength which is approximately 10% (3.0 N/mm^2).

Table 3 Concrete compressive strength f_{cu} of grade C30/37 concrete

7 days compressive strength (4 samples)	
Average weight (kg)	3.60
Average Maximum Load (kN)	213.17
Average Maximum Strength (N/mm^2)	27.14
28 days compressive strength (4 samples)	
Average weight (kg)	3.63
Average Maximum Load (kN)	258.97
Average Maximum Strength (N/mm^2)	32.97

Table 4 Concrete splitting tensile strength f_t of grade C30/37 concrete

7 days splitting tensile strength (4 samples)	
Average weight (kg)	3.61
Average Maximum Load (kN)	92.00
Average Maximum Strength (N/mm^2)	2.93
28 days splitting tensile strength (4 samples)	
Average weight (kg)	3.63
Average Maximum Load (kN)	101.75
Average Maximum Strength (N/mm^2)	3.23

2.3 Experimental Setup

Figure 3 and Figure 4 are the settings of the testing rig. Two rectangular hollow metal with high tensile bolts were fixed on to the testing frame. The dimension of the rectangular hollow metal is 700 × 200 × 550 mm with thickness of 10 mm as support for the column T-block component. Then, the specimen was fastened on the rectangular hollow metal by using bolt and nuts.

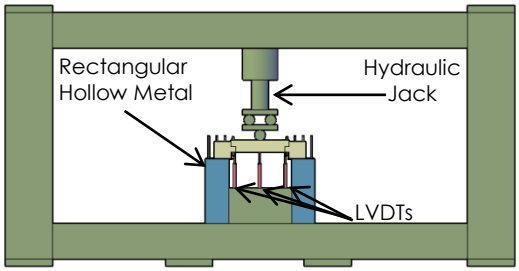

Figure 3 2D view of experimental set-up

Three Linear Variable Displacement Transducers (LVDT) were utilized in this experiment to record the deflection of the specimen. One LVDT was placed at the middle bottom of the beam to measure the maximum mid span deflection and another two LVDTs were placed at both left and right sides below the inter-connection of the corbel to measure movements of the beam-column joint. The actual test set up is shown in the Figure 5.

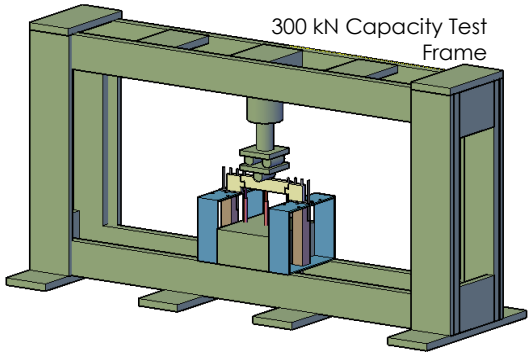

Figure 4 3D view of experiment set-up

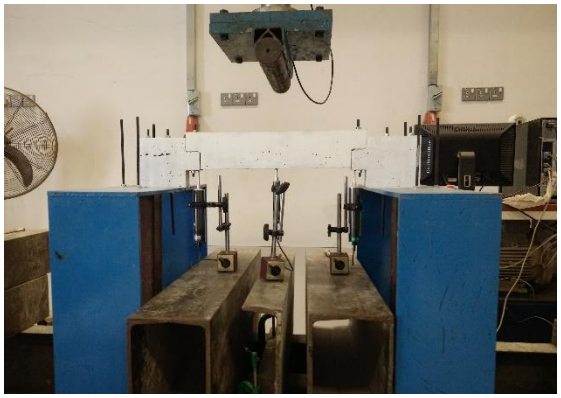

Figure 5 Actual experiment set-up

2.4 Experimental Procedures

Five specimens were prepared in this experimental test. All specimens were tested with single point vertical loads by the structural testing rig shown in Figure 5. All three LVDTs were connected to the data logger to record every minor incremental in displacement.

First three specimens were tested under flexural strength test. Among the three specimens, one control specimen is where the original design column corbel support without any steel anchor plate from Yip *et al*. 2016 [20]. These three specimens are the focus of this research paper to observe the failure behaviour of the joint connection. The applied load was increasing slowly to stabilize the testing frame then increased gradually on to the specimens until the specimen reached the ultimate capacity. Maximum deflection and ultimate load of the specimen at mid span could be obtained by the end of the test. Every 1 kN of load increment with displacement was recorded by LVDTs and stored in data logger. All the cracks and damages were marked on the surface of the specimen during the testing.

Additional two specimens were tested under sudden impact load test. The load was applied on to the specimen until the specimen reached its ultimate capacity instantly. The applied load was recorded every second for this impact load test. Lastly, failure states of all the specimens were extracted for data analysis to obtain the load versus displacement curves and ductility ratio.

3.0 RESULTS AND DISCUSSION

3.1 Load-Displacement of IBS Beam-Corbel for Control Specimen 1

Figure 6 shows the tested load versus displacement chart of control specimen 1. Control specimen 1 is the original design (column corbel without anchor steel plate) done by previous researcher. LVDT 1 and LVDT 3 recorded same displacement along the test due to the balanced load distribution in the loaded specimen. Initially, the load was increasing steadily to stabilize the test specimen on the testing frame and followed by linear increment of the load with displacement. This control specimen was yielded at the load 7 kN with the displacement of 2.1 mm at the mid-span of beam. The linearly increased load with the mid-span displacement from 0 kN to 7.0 kN indicates that the specimen behaved elastically. This specimen was behaved plastically from 7.0 kN to 10.0 kN and strength degradation happend beyond 10 kN. The crushing of concrete corbel at the left side of beam and corbel joint connection with the exposing of steel reinforcement were occurred at 11.0 kN. Hence, this control specimen was failed at 11.0 kN with the mid-span displacement of 7.0 mm.

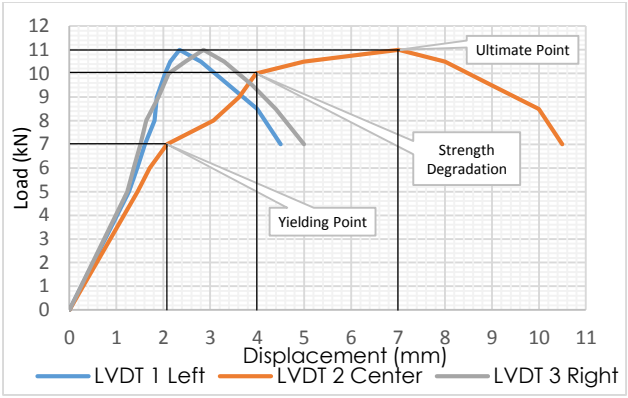

Figure 6 Load vs. displacement for specimen 1 [20]

3.2 Load-Displacement of IBS Beam-Corbel for Specimen 2

Figure 7 shows the load-displacement curve of specimen 2 recorded by LVDT 1, LVDT 2 and LVDT 3. LVDT 1 and LVDT 3 were used to record the displacement at both ends of the beam while LVDT 2 was used to record the mid-span displacement. Theoretically, LVDT 1 and LVDT 3 would record the same displacement during the test due to the same applied load. However, the recorded displacement of LVDT 1 and LVDT 3 does not matched to each other's.

This difference was caused by the stabilization of the whole testing rig. The plotted line for LVDT 1, LVDT 2 and LVDT 3 indicate the load is increasing linearly together with the displacement until the yielding point of the 6.0 kN of load with the mid-span displacement of 2.2 mm. The specimen behaved elastically from 0 kN to 6.0 kN. According to the graph, the specimen 2 was behaved plastically from 6.0 kN to 14.0 kN and strength degradation starts beyond the point of 14.0 kN. The specimen 2 was failed at 15.0 kN with the mid-span displacement of 6.5 mm due to the concrete crushing at the beam joint connection. The strength degradation of the specimen 2 continues with the increasing of deflection after the ultimate point. The newly improved specimen 2 has higher ultimate capacity 15.0 kN against the control specimen 1 with ultimate capacity of 11.0 kN.

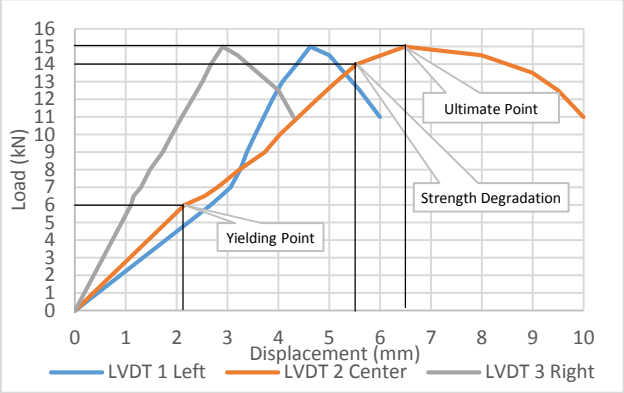

Figure 7 Load versus displacement for specimen 2

3.3 Load-Displacement of IBS Beam-Corbel for Specimen 3

The load versus displacement graph of specimen 3 is illustrated in Figure 8. Based on the graph, LVDT 1 has similar data increment with the LVDT 3. This condition indicates the load was evenly distributed to both end of the beam joint connection. The load is increasing linearly along with the displacement and starts to yield at the load around 6.5 kN with the displacement of 1.9 mm at the mid-span of beam. According to the graph, loads from 6.5 kN to 15.5 kN of the specimen 3 was behaved plastically. The plastic strength degradation started when the load exceeds 15.5 kN. The specimen 3 was failed at 16.0 kN with the mid-span displacement of 6.5 mm due to the crushing of concrete corbel at the left side of beam and corbel joint connection. This specimen has the highest ultimate capacity compared with control specimen 1 and enhanced specimen 2. Specimen 2 and 3 are having same parameter. The reason specimen 3 is higher than specimen 2 is due to the uniform load distribution across the test specimen.

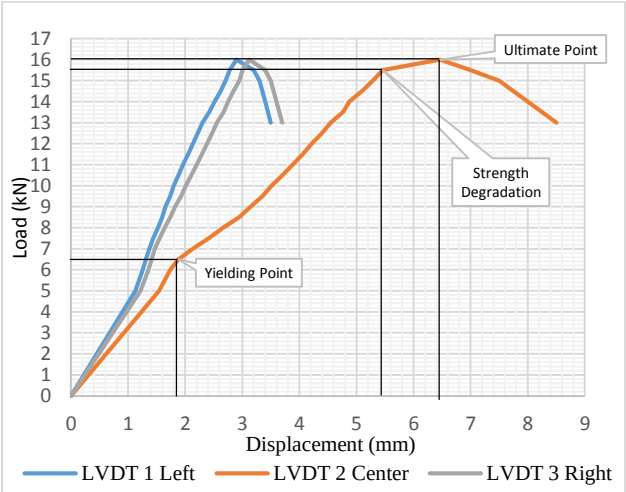

Figure 8 Load versus displacement for specimen 3

3.4 Impact Load Test of Specimen 4 and Specimen 5

The fire explosion or earthquake may damage few parts of the structures. These parts of the structure may break down and impact on the structure below such as slab, beam and column. This phenomena is considered as impact load. Hence, the structural element of the building must have the capability to withstand the sudden impact loads. Specimen 4 and 5 were tested by the sudden applied point load at mid span within time duration of 3 seconds. Figure 9 shows the graph of load (kN) against time (s) for specimen 4. According to the recorded data, the load starts from 0.2 kN at third seconds and increase instantly up to a maximum of 18.0 kN at sixth seconds. Figure 10 shows the graph of load (kN) against time (s) for specimen 5. The initial applied load starts at 0.2 kN at third seconds and the maximum recorded impact load was 16.0 kN at sixth seconds. Both impact loads are close to the tested flexural load capacity.

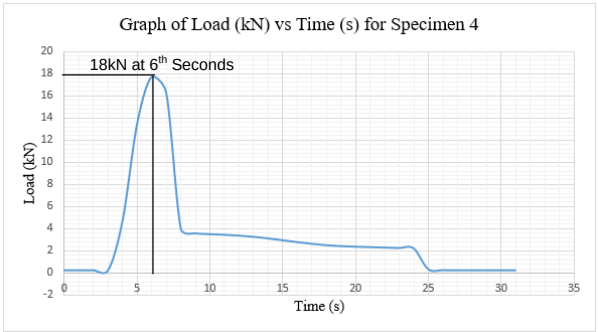

Figure 9 Load versus time for specimen 4

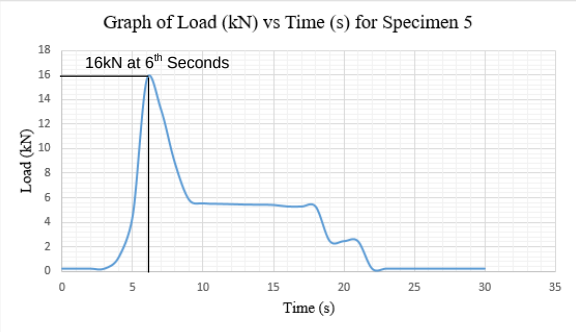

Figure 10 Load versus time for specimen 5

3.5 Cracking Pattern and Mode of Failure

Three types of cracking patterns were found from tested specimens. These cracking were diagonal cracking, shear cracking and flexural cracking. In addition, failure mode such as crushing of concrete corbel was found in this experiment as well.

Initially, point load was applied on the top middle of the beam. The load was distributed to both ends of the beam-column corbel joints connection and then transferred to the base through column T-block. The first cracking was found at the end of the beam joint connection. This is because the distributed load was larger than the tensile strength of the concrete at the beam joint connection. After that, diagonal and shear cracking was appeared at the overlay end due to the high stress concentration at the beam-corbel connection at the corner of reduced section.

Third crack was occurred near to the mid-span of the beam. This pure shear crack has inclination of 45 degrees from the horizontal. This crack was propagated diagonally from the bottom of the beam corbel to the top of the beam. Shear stresses are generated in beams due to bending or twisting. These two types of shear stress are known as flexural shear stress and torsional shear stress respectively. Thus, the shear cracks were developed first then followed by flexural cracks on the beam section.

Fourth crack was formed underneath the beam at the mid span. Pure flexural crack formed at mid span is due to the tensile stress at the tension area of the beam has exceeded the yielding strength of steel and bending strength of reinforced concrete. Thus, the cracking formed straight underneath the loading at the tension area of specimen.

There was crushing of concrete at the beam and corbel joint connection by the end of the experiment. Some parts of the reinforcement were exposed due to crushing of concrete that reached the ultimate strength. Besides, sagging at the mid-span of the beam and a hogging at both end of the beam joint connections were observed as well. The hogging moment at the end of the beam joint connection was caused by the dislocation of the bolt as shown in Figure 11. Due to the high tensile strength bolt, the crushing of concrete at the joint connection has caused a minor bending of the bolt. The specimen was failed when the crushing of concrete and strength degradation with the increasing of deflection at the end of the test. The failure mechanisms are shown in the Figure 12. In summary, the formation of shear cracking and flexural cracking on the beam were found. The corbel connection failed due to the hogging moment and the internal C-shape steel plate reinforcement has anchored the beam from total collapse successfully by the end of this experiment.

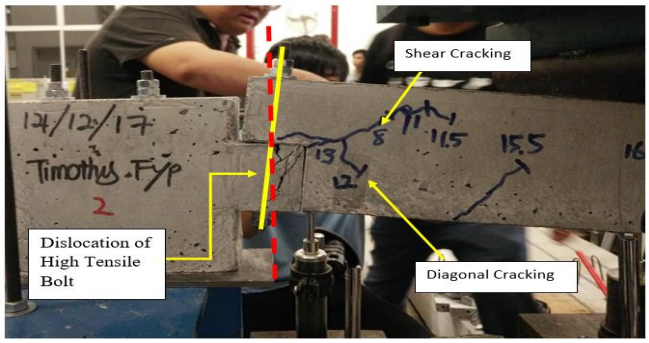

Figure 11 Dislocation of high strength bolt

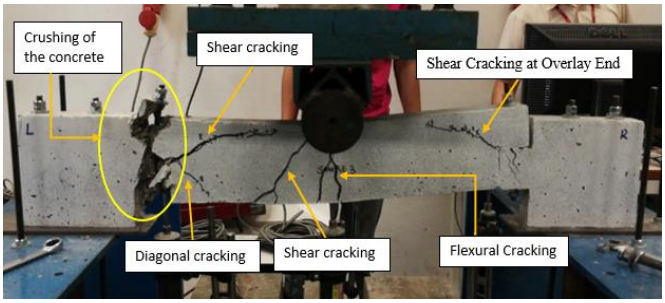

Figure 12 Failure mechanism

3.6 Ductility of IBS Beam Specimen

General definition of ductility is the material's ability to experience the large deformation without rupture before failure [25]. Lestuzzi and Badoux [26] have stated the ductility of reinforced concrete beam can be determined from the ductility factor, *R* which is the ratio between failure displacements to yield displacements. The ductility factor can be computed by using the Eq. 3 as shown below [26].

$$Ductility\ factor\ (R) = \frac{\Delta f}{\Delta y} \quad (3)$$

Where,

Δf = failure displacement,
Δy = yield displacement

Figure 13 shows the deflection profile of the control specimen 1, 2 and 3 at ultimate capacity. Control specimen 1 has the largest deflection at mid span deflection of 7.0 mm follow by specimen 2 & 3 with 6.5 mm only. Large deflection in control specimen 1 is due

to the weak column corbel support. Specimen 2 and 3 have similar ultimate deflection due to enhancement column corbel to support the beam. The yielding displacement is shown in Table 5 to calculate ductility ratio for each of the specimen.

The calculated average ductility ratio is 3.23 which is higher than the pre-stressed concrete beam's ductility ratio of 3.0 specified in PCI design handbook [27]. This indicates that the characteristic of the specimens have higher ductility. The ductility was affected by the factors such as tensile reinforcement ratio, compressive strength of concrete and yield strength of reinforcement [28]. Hence, average of 3.23 ductility ratio greater than standard 3.0 from PCI design handbook 2010 shows this beam-column connection could perform better as an earthquake-resistant structures [27].

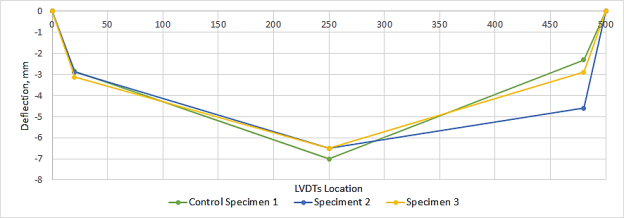

Figure 13 Deflection profile at ultimate capacity

Table 5 Ductility for all specimens

Specimen	Yield Load (kN)	Yield Displacement (mm)	Ultimate Load (kN)	Ultimate Displacement (mm)	Ductility
1	7.0	2.1	11.0	7.0	3.33
2	6.0	2.2	15.0	6.5	2.95
3	6.5	1.9	16.0	6.5	3.42
Average	6.5	2.1	14.0	6.7	3.23

3.7 Summary of Result

Figure 14 shows the combined results for comparisons among control specimens 1, specimen 2 and specimen 3 for. Control specimen 1 has the lowest ultimate capacity of 11.0 kN compared to the enhanced beam-column connection specimen 3 with the highest ultimate capacity of 16.0 kN.

Besides, the elastic stiffness for specimen 1, 2 and 3 are 3.4 kN/mm, 2.8 kN/mm and 3.3 kN/mm, respectively. All three specimens have similar elastic stiffness at the beginning of the experiment. As for the load was progressively applied on to the specimen, the post elastic stiffness for these specimen 1, 2 and 3 are 1.2 kN/mm, 2.8 kN/mm and 3 kN/mm, respectively. The stiffness of control specimen 1 starts to reduce due to the formation of cracks and damages found at beam-column connection. Finally, the plastic stiffness for specimen 1, 2 and 3 are 0.3 kN/mm, 1.0 kN/mm and 0.4 kN/mm, respectively. Although, the specimen 3 has the highest ultimate capacity but its full plastic stiffness is similar with the controlled specimen 1. The reason is due to similar failure mechanism when the formation of plastic hinge happen around the beam corbel connection.

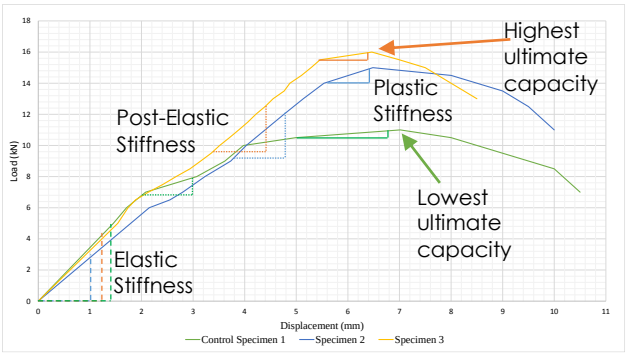

Figure 14 Flexural capacity of specimen 1, 2 and 3

Figure 15 shows the combined results of impact load test in terms of load (kN) against time (s) for specimen 4 and specimen 5. The specimen 4 managed to sustain the maximum sudden load, which is 18.0 kN while the specimen 5 was sustained to 16.0 kN. Both specimens were able to withstand minimum tested control specimen 1 flexural strength of 11.0 kN because these two enhanced beam-column corbel connection does not undergoes stiffness degradation due to the slow applied load. Thus, this research is successful in terms of ultimate strength enhancement, post elastic stiffness improvement and protective anchorage from total collapse behaviour.

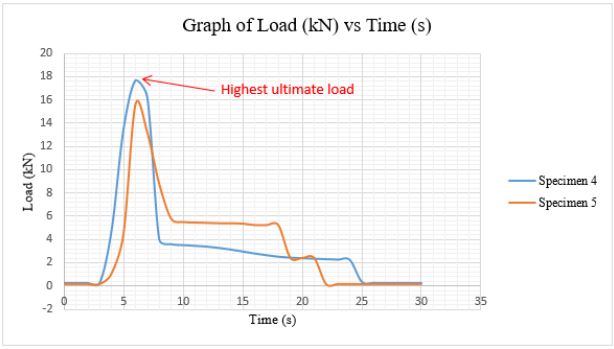

Figure 15 Impact load test for specimen 4 and 5

Table 6 shows the summary of the tested results. Few highest parameters were selected to determine the full scale specimen capacity by multiplying the scale factor. The highest ultimate displacement from control specimen 1 with 7.0 mm has full scale deflection of 35.0 mm after the multiplication of scaling factor. 18.0 kN of ultimate load from specimen 4 has a full scale flexural load resistance of 2025.0 kN. Highest yield load from control specimen 1 has full scale capacity of 787.5 kN. The highest elastic, post-elastic and plastic stiffness have full scale capacity of 76.5 kN/mm, 67.5 kN/mm, and 22.5 kN/mm,

respectively. The 1:5 scaled flexural strength is using basic simply supported equation PL/4 with P = 18 kN of ultimate load and length of 0.5 m to obtain 2.2kNm. The projected flexural strength of full scaled beam has 1265.6 kNm with the multiplication of scaled factor of S_eS^3.

Table 6 Summary of result

Specimen	Yield Load (kN)	Yield Displacement (mm)	Ultimate Load (kN)	Ultimate Displacement (mm)
1	7.0	2.1	11.0	7.0
2	6.0	2.2	15.0	6.5
3	6.5	1.9	16.0	6.5
4	-	-	18.0	-
5	-	-	16.0	-
Parameter		**Scale factor**	**Scaled 1:5**	**Full Scale 1:1**
Dimension		$S = 5.0$	0.2	1.0
Material strength		$S_e = 4.5$	0.22	1.0
Highest Ultimate displacement, (mm)		$S = 5.0$	7.0	35.0
Highest Yielding displacement, (mm)		$S = 5.0$	2.2	11.0
Highest Ultimate load, (kN)		$S_eS^2 = (4.5)(5.0)^2$	18.0	2025.0
Highest Yielding load (kN)		$S_eS^2 = (4.5)(5.0)^2$	7.0	787.5
Highest elastic Stiffness, K_i (kN/mm)		$S_eS = (4.5)(5.0)$	3.4	76.5
Highest Post elastic Stiffness, K_i (kN/mm)		$S_eS = (4.5)(5.0)$	3	67.5
Highest plastic Stiffness, K_i (kN/mm)		$S_eS = (4.5)(5.0)$	1.0	22.5
Flexural Strength (kNm)		$S_eS^3=(4.5)(5.0)^3$	2.2	1265.6

4.0 CONCLUSIONS

The finding of the failure behaviour for these specimen are starting with flexural crack at the mid span followed by shear cracks at the beam support and ends with crushing of the beam corbel connection to the concrete column's supports. The progressive deformation gave an insight for the engineer from industry to design the IBS beam with better flexural resistance.

The flexural strength of scaled 1:5 specimen has 2.2 kNm with maximum deflection of 7.0 mm. The projected full scale specimen may have 1265.6 kNm within the mid span of the 2.5 m length beam. Thus, the projected data allows the structural design engineer to a ratio equation for calculating the theoretical bending moment at mid span with different in length.

The ductility and strength of joint connection strength was influenced by three factors, which are the compressive strength of concrete, yield strength and ultimate strength of reinforcement. The tested specimen has differential in strength of 6%-12% with the median of 16 kN ultimate capacity. Thus, controlling the size of the beam-column corbel support in the future would significantly improve the strength and failure behaviour.

The loaded specimens are behaving elastically followed by plastically and ends with plastic strength degradation with highest specimen's stiffness 3.4 kN/mm, 3 kN/mm and 1.0 kN/mm at each state, respectively. Thus, the beam was deformed in stages; with the increasing of applied load the stiffness of the beam reduces and eventually the plastic hinge was formed at the connection support before total collapse.

The calculated ductility ratio for these scaled specimens has the average of 3.23 but one of the specimen has lowest ductility ratio 2.95 which is still within the range of 3.0 ductility as specified by PCI design handbook [27]. Other specimen with the value higher than the 3.0 could withstand longer during the earthquake event. Flexural and shear cracking will occur on the beam before the crushing of the beam and corbel's connection joints. Hence, the micro damage can give the signal to the occupants to escape from the building before collapse.

This research shows the control specimen has ultimate capacity of 11kN and the newly improved specimen has average ultimate capacity of 16.2kN. This outcome shows the newly improved beam-column joint connection has the load bearing improvement of 32%. Thus, this research has positive outcome that could improve the confident of the industry user to produce better structural system.

Acknowledgement

Authors express gratitude to Universiti Tunku Abdul Rahman and its facilities which makes this important research viable and effective.

References

[1] Lachimpadi, S. K., Pereira, J. J., Taha, M. R. and Mokhtar, M. 2012. Construction Waste Minimisation Comparing Conventional and Precast Construction (Mixed System and IBS) Methods in High-rise Buildings: A Malaysia Case Study. *Journal of Resources, Conservation and Recycling*. 68(1): 96-103.

[2] Kamar, K. A. M., Hamid, Z. A. and Din, I. 2012. The Adoption of Industrialised Building System (IBS) Construction in Malaysia. *Journal of Gerontechnology*. 11(2).

[3] Wah, P. L., Razali, A. K., M., Saleh, J. M. and Sapuan, S. M. 2003. The Essential Characteristics of Industrialised Building System. *International Conference on Industrialised Building Systems*. 283-292.

[4] CIDB. 2003. *Industrialised Building Systems (IBS) - Roadmap 2003-2010*. Malaysia.

[5] Othuman Mydin, M. A., Sani, N. M. and Taib, M. 2014. Industrialised Building System in Malaysia: A Review. *MATEC Web of Conferences*. 10(P01002).

[6] Kamar, K. and Hamid, Z. 2011. Industrialised Building System (IBS): Revisiting Issues of Definition and Classification. *International Journal of Engineering*. 1(1): 120-132.

[7] Ning, N., Qu, W. and Ma, Z. J. 2016. Design Recommendations for Achieving Strong Column-Weak Beam in RC Frames. *Journal of Engineering Structures*. 126(1): 343-352. DOI: 10.1016/j.engstruct.2016.07.053.

[8] Nam, S. K., Ji, H. L. and Sung, P. C. 2009. Equivalent Multi-Phase Similitude Law for Pseudo-dynamic Test On Small Scale Reinforced Concrete Models. *Journal of Engineering Structure*. 31: 834-846. Elsevier.

[9] Andreas, S., Benson. S, and Joel, C. 2010. Design, Scaling, Similitude and Modelling of Shake Table Test Structures. Shake Table Training Workshop 2010. *29th September 2010. National Earthquake Hazards Reduction Programme*.

University of California, San Diego, CA. 1-52.
[10] Mehta, P. K. and Monteiro, P. J. M. 2013. *Concrete: Microstructure, Properties, and Materials*. 4th Edition. McGrawHill: United State.
[11] Cement Concrete & Aggregates Australia (CCAA). 2004. *Concrete Basics: A Guide to Concrete Practice*. 6th Edition. CCAA: Australia.
[12] BS EN 934. 2009. *Admixtures for Concrete, Mortar and Grout*. British Standards Institution: London.
[13] Okamura, H. and Ouchi, M. 2003. Self-Compacting Concrete. *Journal of Advanced Concrete Technology*. 1(1): 5-15.
[14] Zhou, K. J. H., Ho, J. C. M. and Su, R. K. L. 2011. Flexural Strength and Deformability Design of Reinforced Concrete Beams. *Procedia Engineering*. 14(1):1399-1407.
[15] Kwan, A. K. H., Ho, J. C. M. and Pam, H. J. 2002. Flexural Strength and Ductility of Reinforced Concrete Beams. *Proceedings of the Institution of Civil Engineers: Structures and Buildings*. 152(4): 1-9.
[16] Yip, C. C., Marsono, A. K., Wong, J. Y., Lee, S. C. 2017. Seismic Performance of Scaled IBS Block Column for Static Nonlinear Monotonic Pushover Experimental Analysis, *Journal of Engineering & Science*. Jurnal Teknologi. 80(1): 89-106. DOI: https://doi.org/10.11113/jt.v80.10799.
[17] Murugan, R., Prabhu, R. V., and Thyla, P. R. 2013. Establisment of Structural Similitude for Elastic Models and Validation of Scaling Laws. *Journal of Civil Engineering*. 17(1): 139-144. Springer.
[18] Helmut, K. and Eduardo, M. 2004. *Performance Based Earthquake Engineering*. Stanford, California: CRC Press LLC.
[19] Yip, C. C., Marsono, A. K., Wong, J. Y. and Mugahed, Y. H. A. 2015. Flexural Strength of Special Reinforced Lightweight Concrete Beam for Industrialised Building System (IBS), *Journal of Engineering and Science*. Jurnal Teknologi. 77(1): 187-196. DOI: https://doi.org/10.11113/jt.v77.3505.
[20] Yip, C. C. and Marsono, A. K. 2016. Structural Seismic Performance of Reinforced Concrete Block System for Two Storeys Safe House. *Journal of Engineering and Science*. Jurnal Teknologi. 78(2): 83-97. DOI: https://doi.org/10.11113/jt.v78.5098.
[21] BS EN 1992-1-1. 2004. *Eurocode 2: Design of Concrete Structures - Part 1-1 : General Rules and Rules for Buildings*. British Standards Institution: London.
[22] British Standard Institution. 1992. *European Code 3: Design of Steel Structure*. British Standards Institution: London.
[23] British Standard Institution. 2000. *B.S. 5950: Structural Use of Steelwork in Building*. British Standards Institution: London.
[24] British Standard Institution. 1997. *BS5328: Method of Specifying Concrete Mixes*. British Standards Institution: London.
[25] Duggal, S. K. 2013. *Earthquake - Resistant Design of Structures*. 1st Edition. CIVILAX: Philipine.
[26] Lestuzzi, P. and Badoux, M. 2003. The Gamma-model: A Simple Hysteretic Model for Reinforced Concrete Walls. *Proceeding of the fib-Symposium: Concrete Structures in Seismic Regions*. 1-12.
[27] Shaikh, A. F. 2010. *PCI Design Handbook-Precast and PreStressed Concrete*. Precast/Prestressed Concrete Institute: United States of America.
[28] Guray, A. and Ercan, C. 2010. Curvature Ductility Prediction of Reinforced High Strength Concrete Beam Sections. *Journal of Civil Engineering and Management*. 16(4): 462-470. DOI: https://doi.org/10.3846/jcem.2010.52.